

Supporting Information for: A Theranostic Gallium Siderophore Ciprofloxacin Conjugate with Broad Spectrum Antibiotic Potency.

Apurva Pandey,^a Chloé Savino,^a Shin Hye Ahn^a, Zhaoyong Yang,^b Steven G. Van Lanen^c and Eszter Boros^{a,*}

^aDepartment of Chemistry, Stony Brook University, 100 Nicolls road, Stony Brook, New York, 11790, United States

^bInstitute of Medicinal Biotechnology, Chinese Academy of Medical Sciences and Peking Union Medical College, Beijing 100050, People's Republic of China

^cDepartment of Pharmaceutical Sciences, College of Pharmacy, University of Kentucky, Lexington, Kentucky 40536, United States

Table of Contents

1. Chemical Synthesis and Characterization
 - 1.1 NMR Spectra
2. Characterization of Conjugate Complexes Employed in Biological Testing
 - 2.1 HPLC Purity Analyses
 - 2.2 UV-VIS Data
3. Radiochemistry
 - 3.1 RadioHPLC traces
 - 3.2 Radiochemical Complex Challenge Assays
 - 3.3 Relative Complex Inertness Experiments
 - 3.4 Radiochemical Complex Uptake in *E. coli* K-12
 - 3.5 Challenge Uptake Assay in wt. *E. coli* K-12
4. Antibacterial Potency Assays
 - 4.1 MIC Assay Results of Siderophores with *E. coli*
 - 4.2 Challenge MIC Assays
 - 4.3 MIC Assay Results with *E. coli* (AN 193)
 - 4.4 MIC Assay Results with *P. aeruginosa* (PA01)
 - 4.5 MIC Assay Results with *S. aureus newman* (RN 4220)
 - 4.6 MIC Assay Results with *K. pneumoniae* (CRE-11)
 - 4.7 MIC Assay Results with Fe-D3 (albomycin) in Different Bacterial Strains
5. Animal Studies
 - 5.1 Biodistribution
 - 5.2 Metabolite Analysis

1. Chemical Synthesis and Characterization

1.1 NMR Spectra

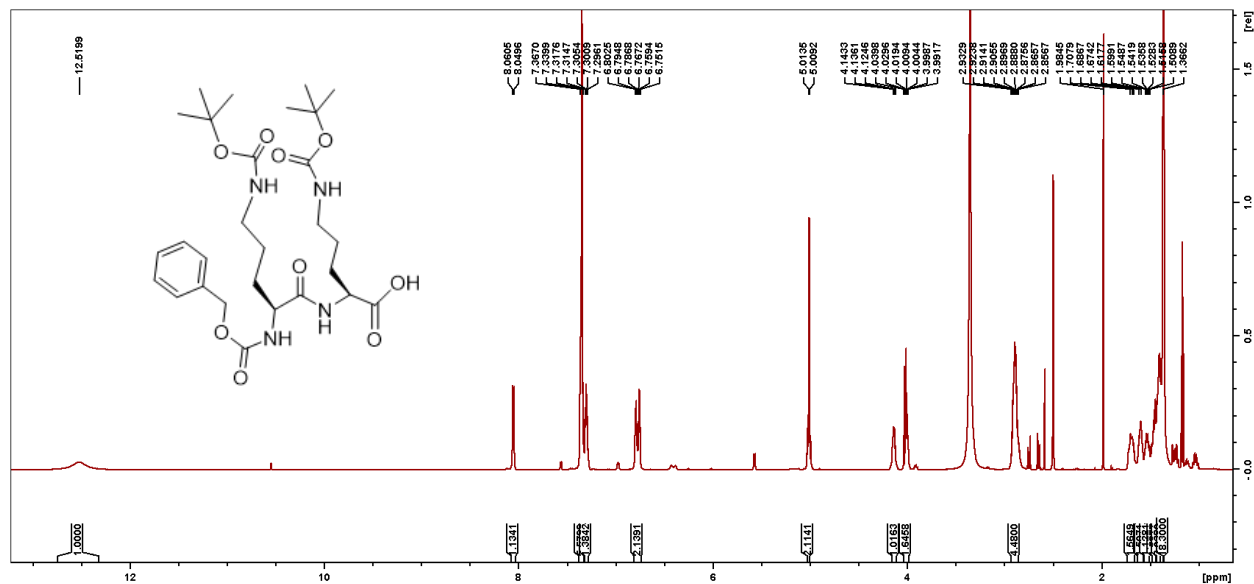


Figure S1 ¹H NMR spectrum of P1.

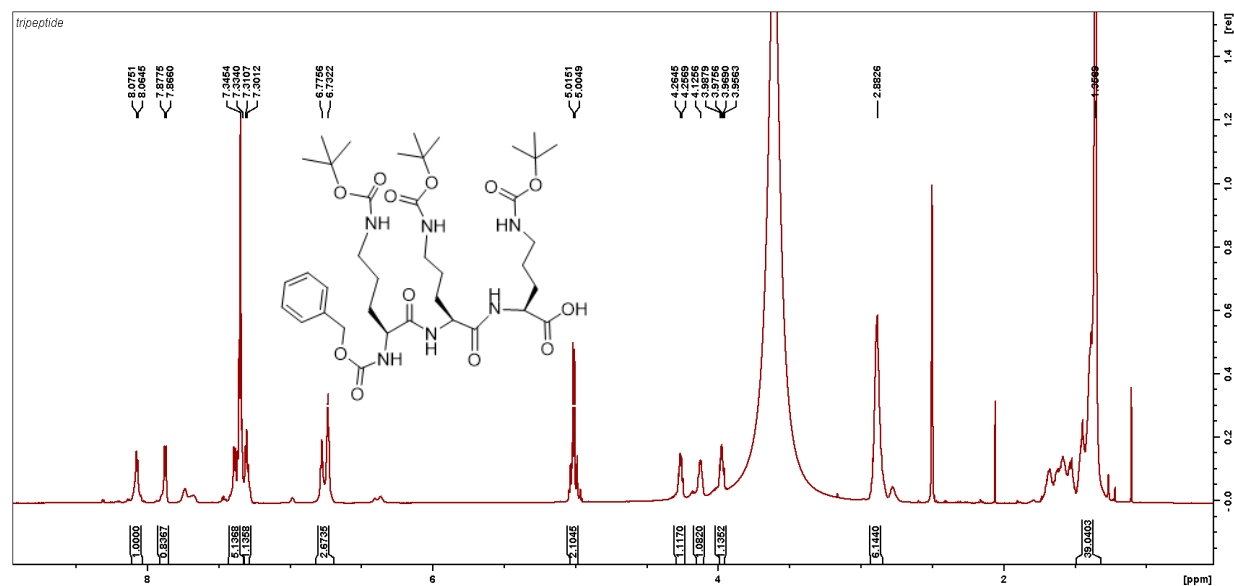


Figure S2: ¹H NMR spectrum of P2.

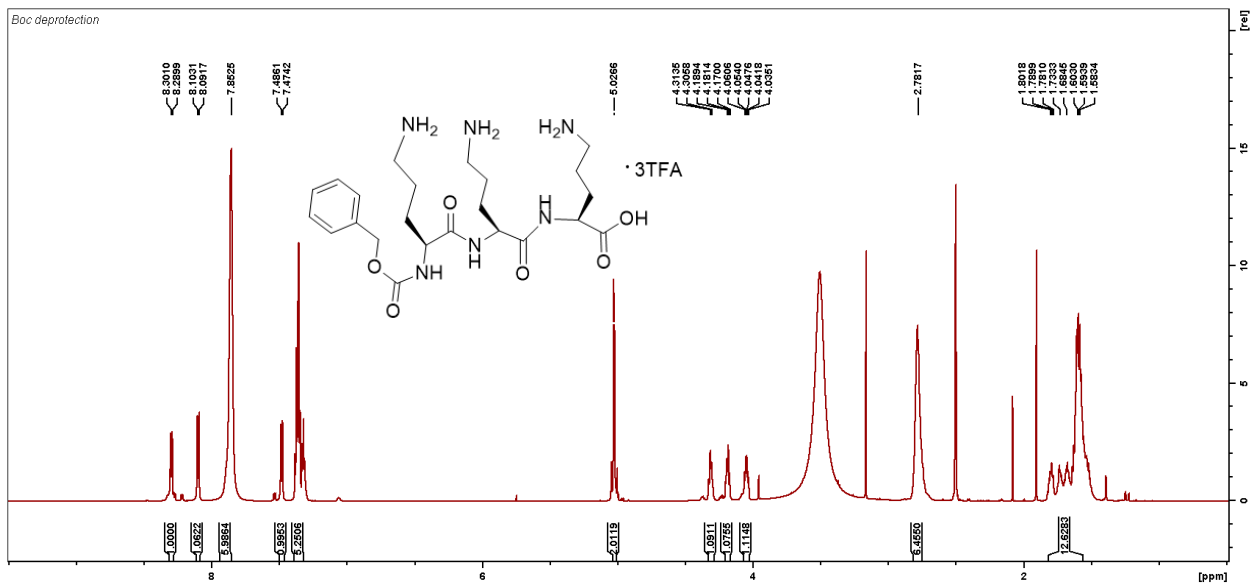


Figure S3: ¹H NMR spectrum of P3.

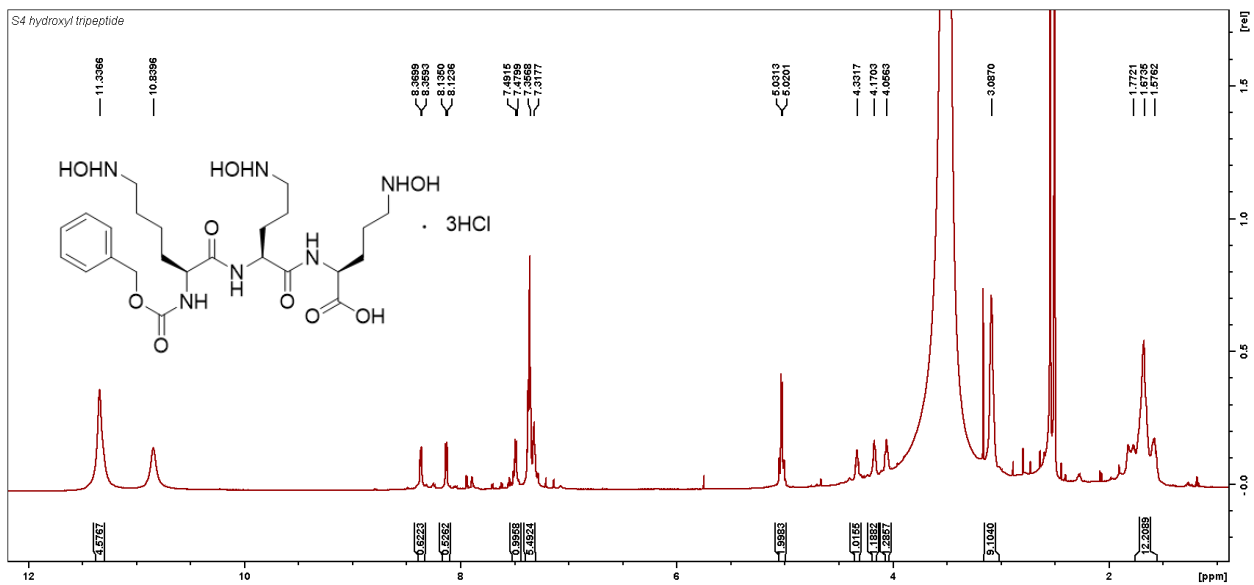


Figure S4: ¹H NMR spectrum of P4.

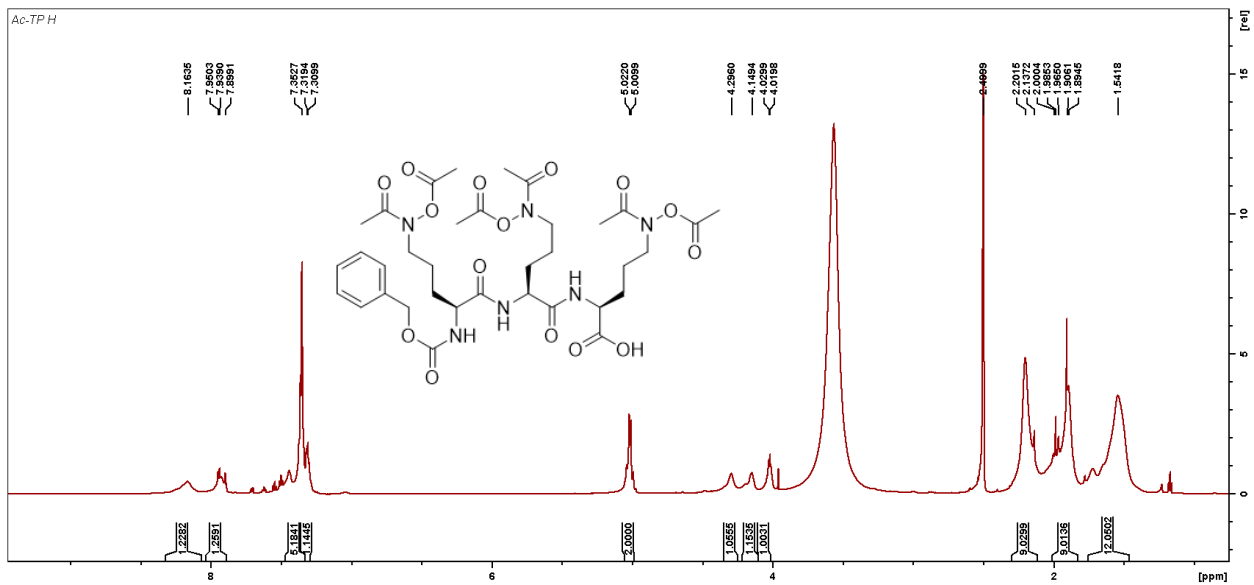


Figure S5: ^1H NMR spectrum of P5.

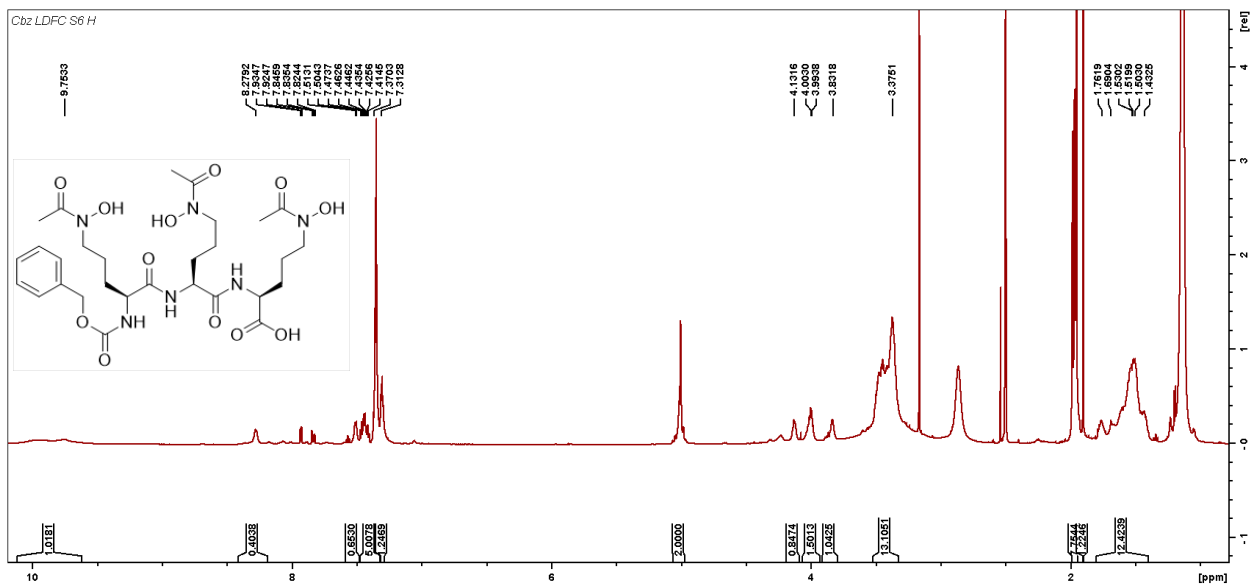


Figure S6: ^1H NMR spectrum of A1.

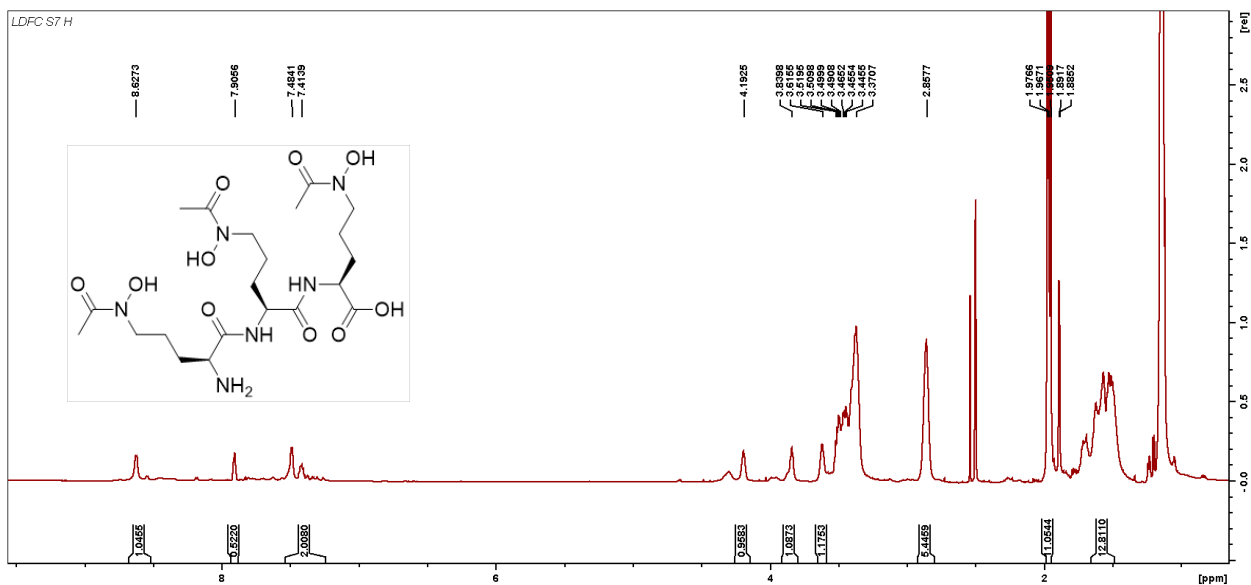


Figure S7: ^1H NMR spectrum of A2.

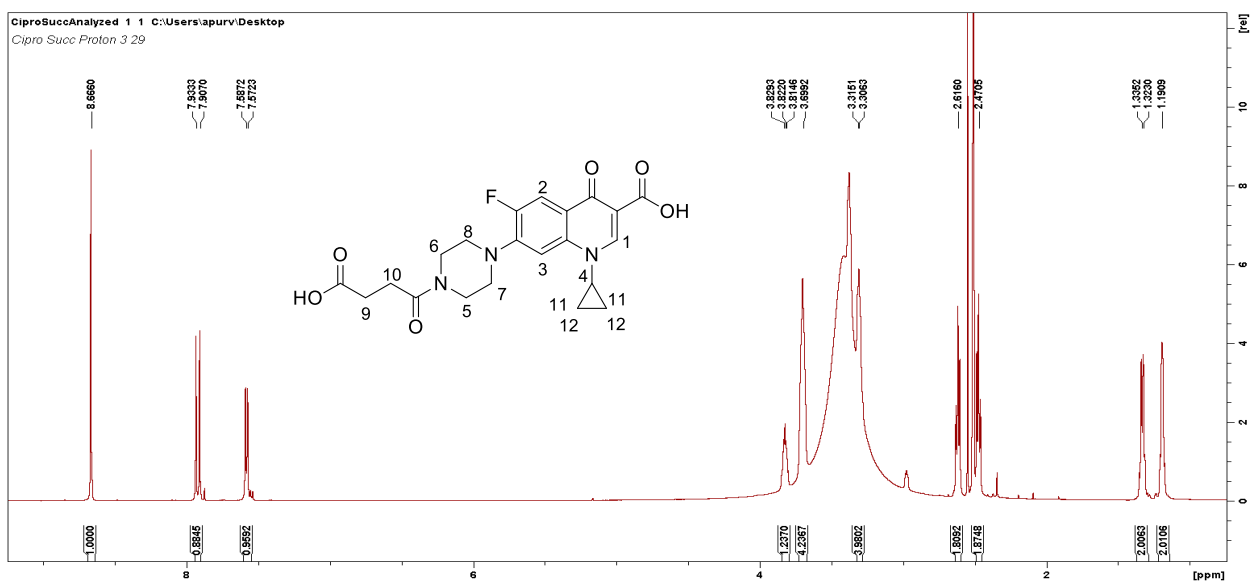


Figure S8: ^1H NMR spectrum of C1.

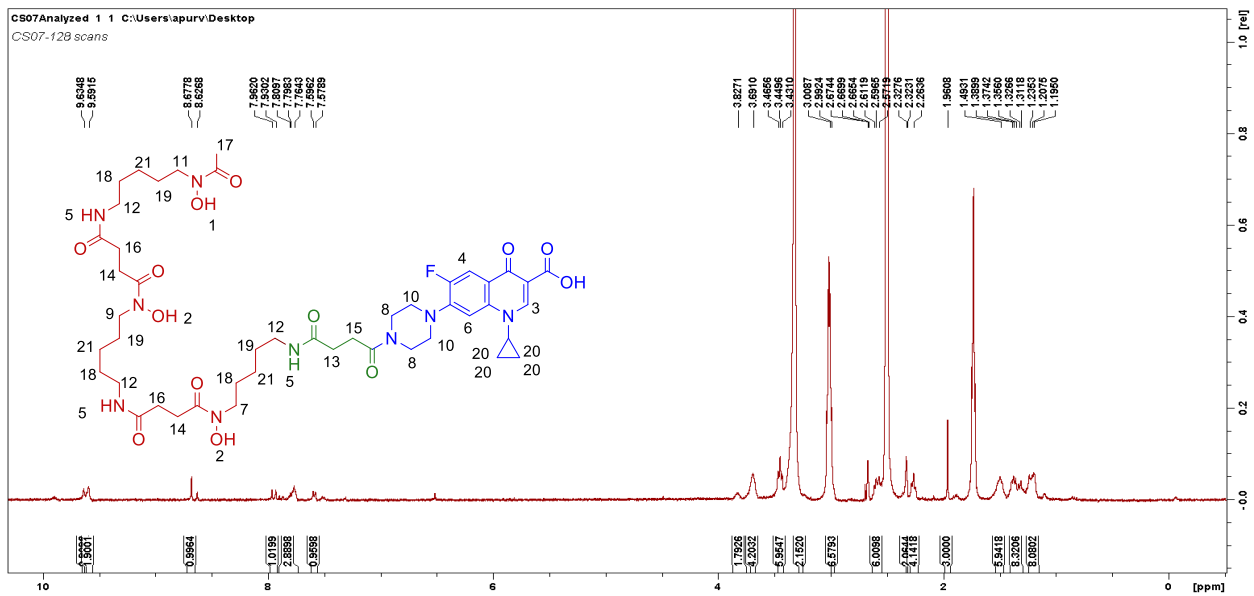


Figure S9: ^1H NMR spectrum of **D1**.

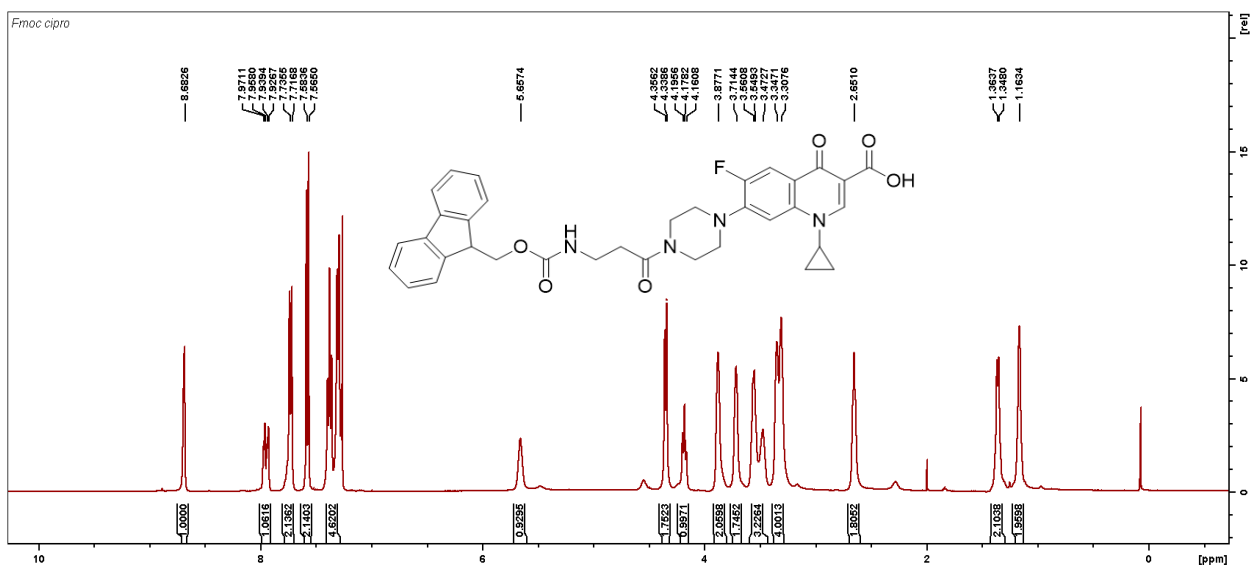


Figure S10: ^1H NMR spectrum of **B1**.

2. Characterization of Conjugate Complexes employed in biological testing

2.1 HPLC Purity analyses

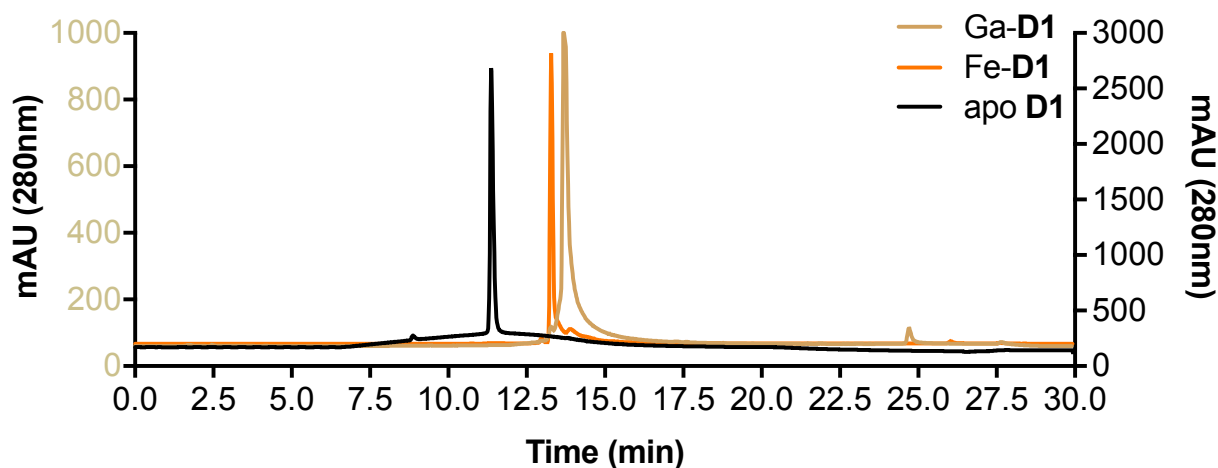


Figure S13: HPLC traces of **D1** ($R_t = 11.5$ min) and its Fe ($R_t = 13.28$ min) and Ga ($R_t = 13.85$ min) complex. Purity of complex species: apo-**D1**: 99.1 %, Ga-**D1**: 98.7%, Fe-**D1**: 95.6%.

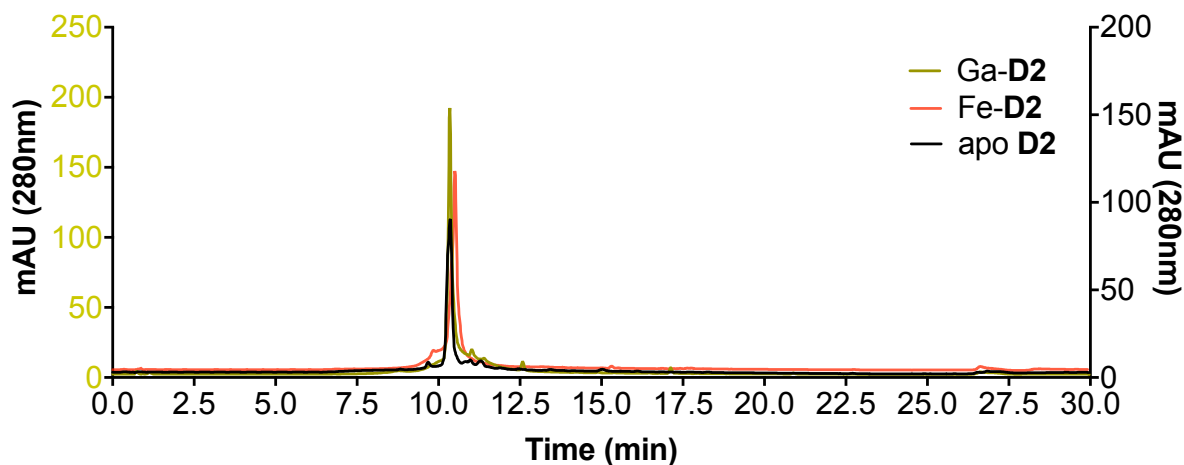


Figure S14: HPLC traces of **D2** ($R_t = 10.30$ min) and its Fe ($R_t = 10.50$ min) and Ga ($R_t = 10.37$ min) complex. Purity of complex species: apo-**D2**: 95.6%, Ga-**D2**: 98.7%, Fe-**D2**: 97.3%.

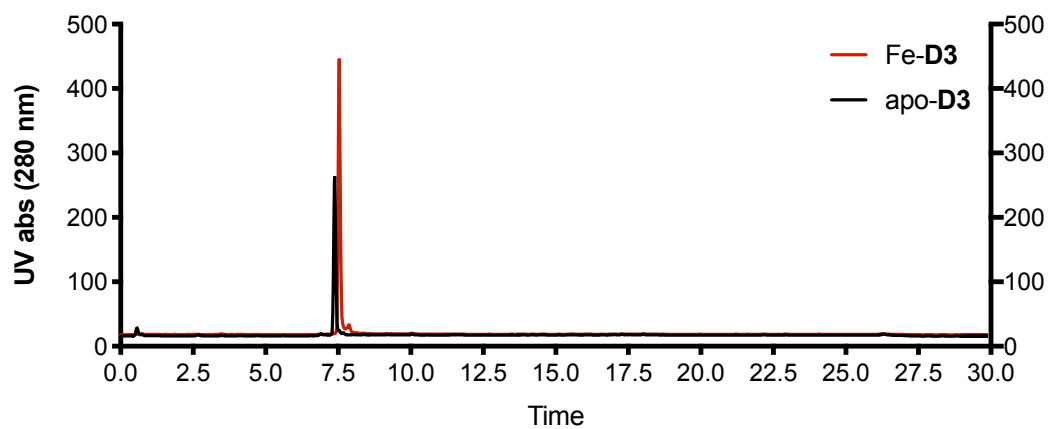


Figure S15: HPLC traces of **D3** ($R_t = 7.35$ min) and its Fe ($R_t = 7.53$ min) complex. Purity of complex species: apo-**D3**: 96.4%, Fe-**D3**: 98.8%.

2.2 UV-VIS Plots

UV-VIS spectra were collected with the NanoDrop ¹C instrument (AZY1706045). Spectra were recorded from 200 to 600 nm in a quartz cuvette with 1 cm path length. All samples except apo **D1** (<1 % DMSO) were dissolved in water.

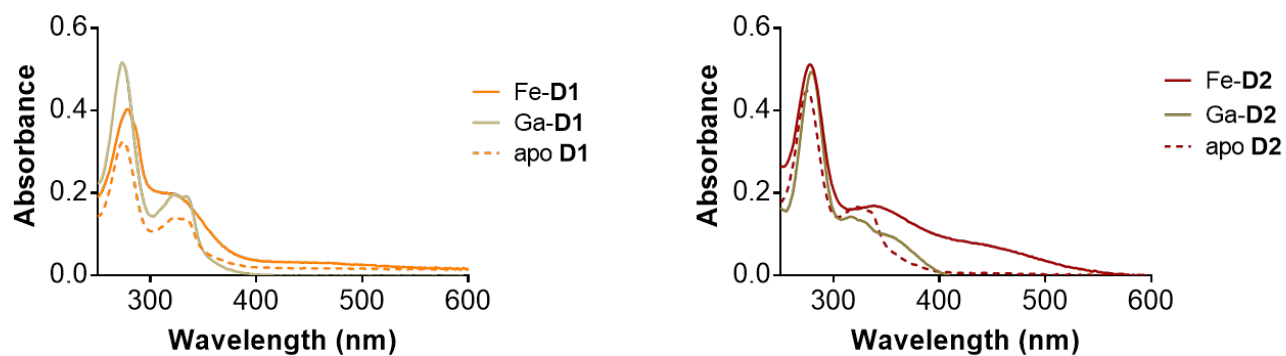


Figure S16: UV-VIS spectra for (left) **D1** and (right) **D2** complexes.

3. Radiochemistry

3.1 RadioHPLC traces

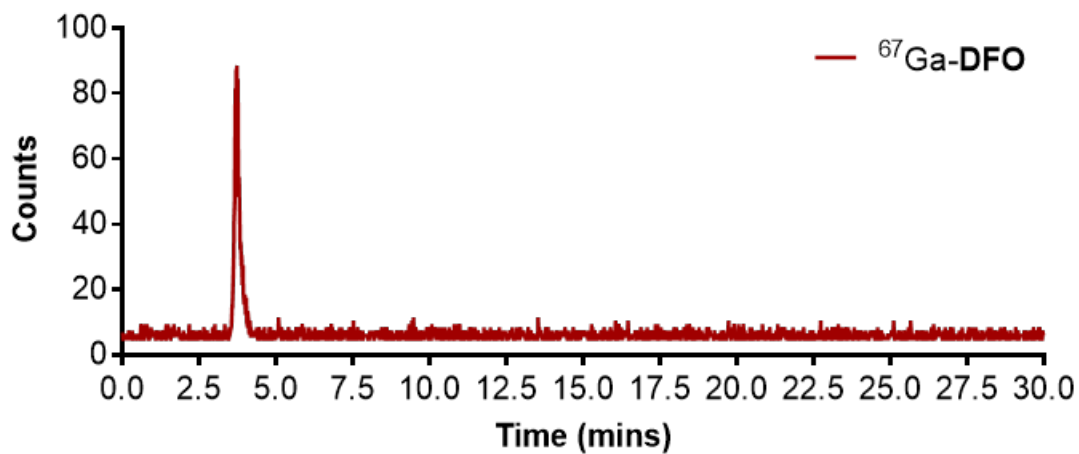


Figure S17: Radio HPLC trace of $^{67}\text{Ga-DFO}$ ($R_t = 3.72$ min). Purity of complex species: >99%.

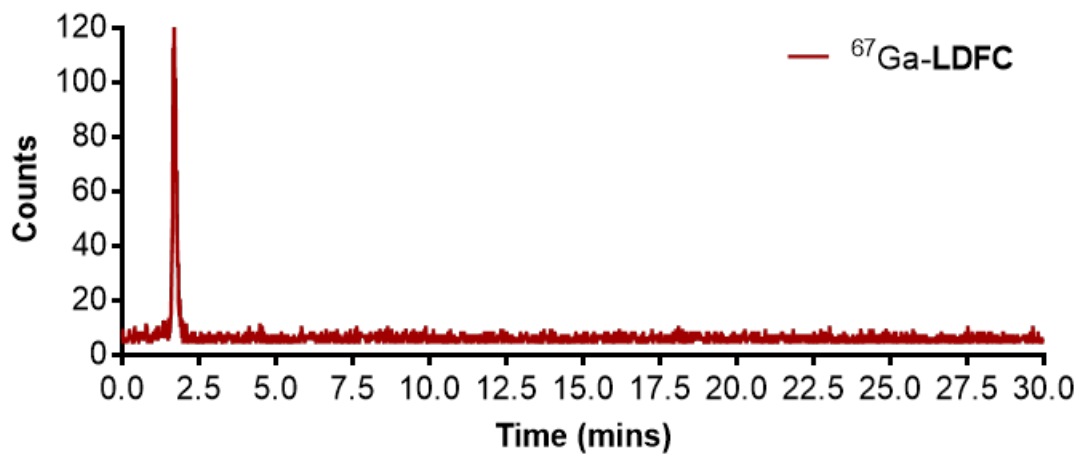


Figure S18: Radio HPLC trace of $^{67}\text{Ga-LDFC}$ ($R_t = 1.65$ min). Purity of complex species: >99%.

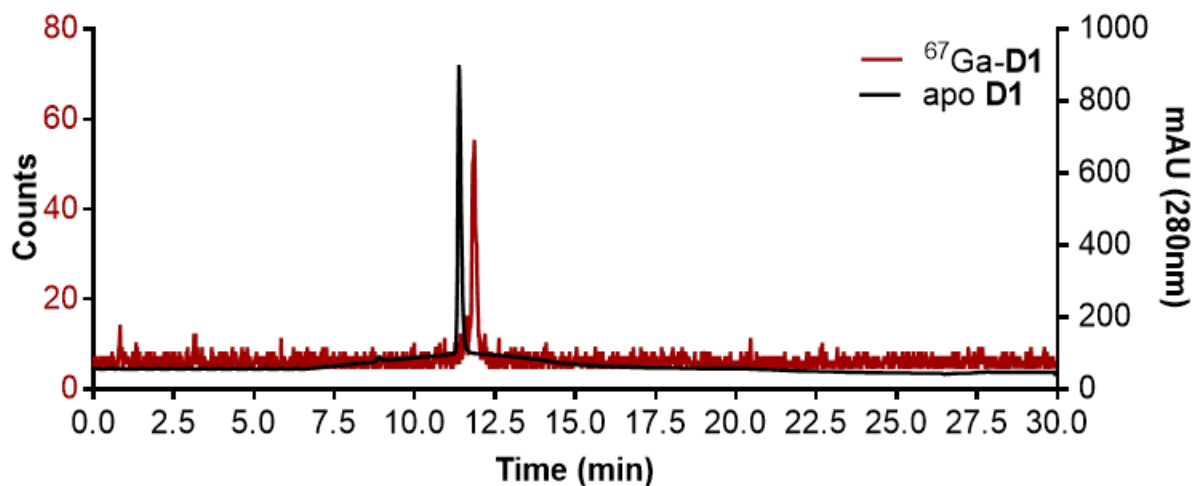


Figure S19: Radio HPLC and UV trace of $^{67}\text{Ga-D1}$ ($R_t = 13.85$ min). Purity: apo-D1: 99.1 %, $^{67}\text{Ga-D1}$: 99%.

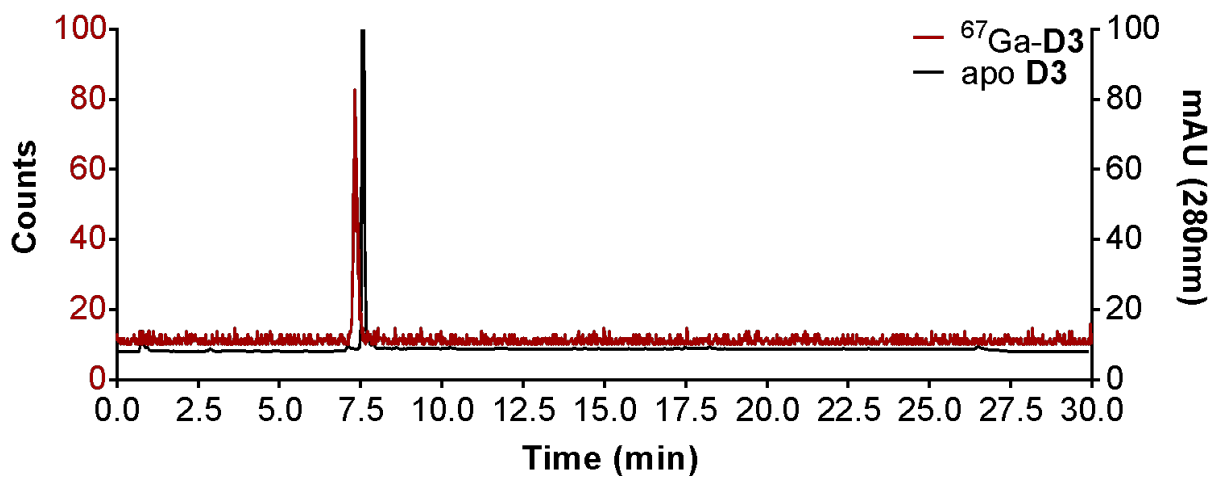


Figure S20: Radio HPLC and UV trace of $^{67}\text{Ga-D3}$ ($R_t = 7.27$ min). Purity: apo-D3: 96.4 %, $^{67}\text{Ga-D3}$: 99 %.

3.2 Radiochemical Complex Challenge Assays

Table S1: Percentage of intact ^{67}Ga complexes upon incubation with 10 fold excess EDTA.

Incubation Time (h)	$^{67}\text{Ga-DFO}$ (%)	$^{67}\text{Ga-LDFC}$ (%)	$^{67}\text{Ga-D1}$ (%)	$^{67}\text{Ga-D2}$ (%)	$^{67}\text{Ga-D3}$ (%)
0	100	100	100	100	100
0.16	100	50 ± 6	100	50	71 ± 18
0.33	100	41 ± 5	80	32 ± 8	60
0.5	100	27 ± 7	75 ± 3	19	45 ± 1
1	90	12 ± 2	72	13	37 ± 1
2	78 ± 1	0	60 ± 1	0	20 ± 1

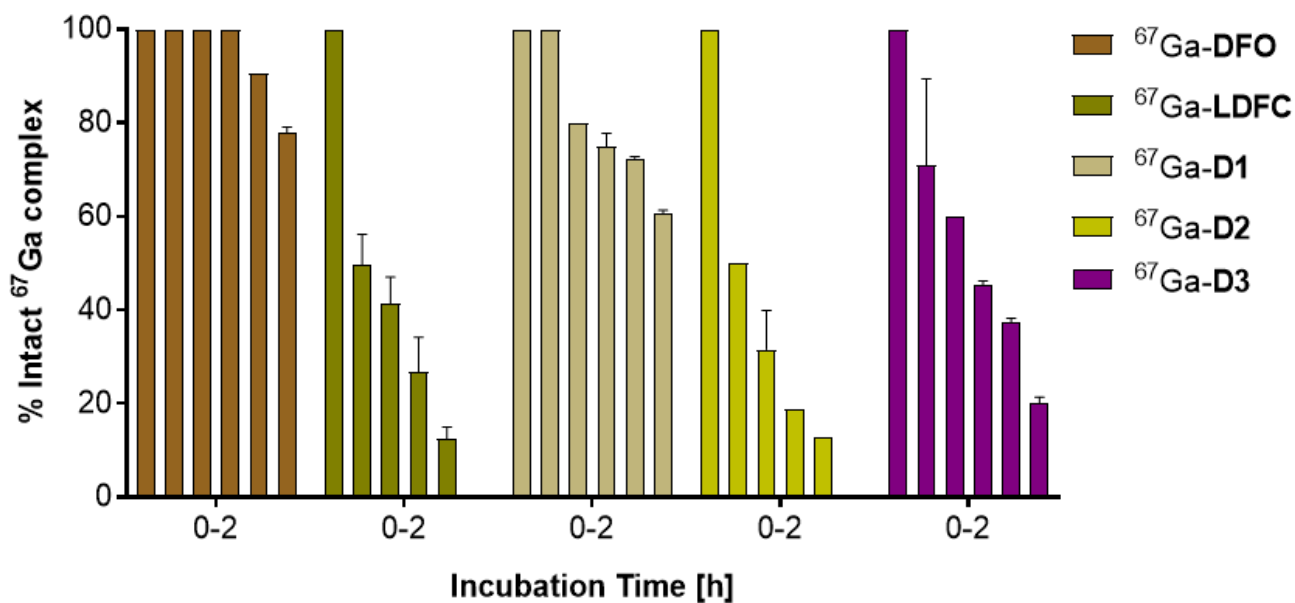


Figure S21: Bar graph plot of results of the 10-fold excess EDTA challenge; complex integrity is expressed as percentage of intact siderophore complex and time upon incubation in EDTA (n=3).

3.3 Relative Complex Inertness Experiments

To assess the stability of complexes in LB broth, challenge experiment was carried out with iron sufficient and iron deficient LB Broth (0.8 mL of a 1 mg/mL sterile aq. solution of 2,2'-bipyridine to 49.2 mL of LB) in duplicates. ^{67}Ga complexes were incubated with equal volume of LB. The transchelation was monitored every 10 min, 20 min, 30 min, 1 h and 2 h by radio HPLC, method A.

^{67}Ga complexes of hydroxamate-based siderophores and sideromycins behaved as follows:

$$^{67}\text{Ga-DFO} = ^{67}\text{Ga-LDFC} = ^{67}\text{Ga-D1} = ^{67}\text{Ga-D3} > ^{67}\text{Ga-D2}.$$

Table S2: Percentage of intact ^{67}Ga complexes upon incubation with iron sufficient LB broth.

Incubation Time (h)	$^{67}\text{Ga-DFO}$ (%)	$^{67}\text{Ga-LDFC}$ (%)	$^{67}\text{Ga-D1}$ (%)	$^{67}\text{Ga-D2}$ (%)	$^{67}\text{Ga-D3}$ (%)
0	100	100	100	100	100
0.16	100	100	100	100	100
0.33	100	100	100	100	100
0.5	100	100	100	85	100
1	100	100	100	84	100
2	100	100	100	70	100

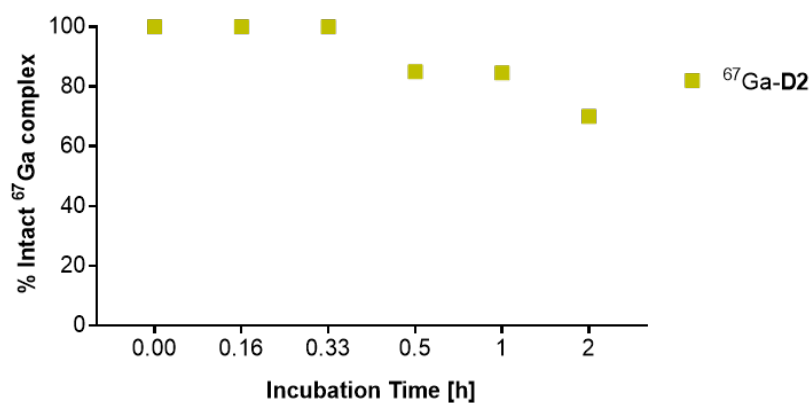


Figure S22: Scatter plot results for complexes that lost integrity in iron sufficient LB broth; complex integrity is expressed as percentage of intact complex and time upon incubation in iron sufficient LB broth (n=3).

Table S3: Percentage of intact ^{67}Ga complexes upon incubation with iron deficient LB broth.

Incubation Time (h)	^{67}Ga -DFO (%)	^{67}Ga -LDFO (%)	^{67}Ga -D1 (%)	^{67}Ga -D2 (%)	^{67}Ga -D3 (%)
0	100	100	100	100	100
0.16	100	100	100	100	85
0.33	100	100	100	74±1	85
0.5	100	100	100	71	84
1	100	100	100	76±1	84
2	100	100	100	70	84

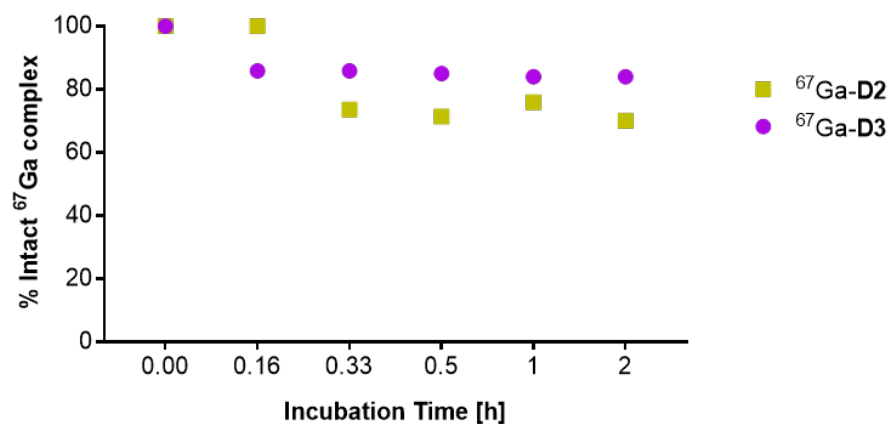


Figure S23: Scatter plot results for complexes that lost integrity in iron deficient LB broth; complex integrity is expressed as percentage of intact complex and time upon incubation in iron deficient LB broth (n=3).

3.4] Uptake of ^{67}Ga Labeled Ciprofloxacin-Conjugates by *E. coli* K-12

Uptake was expressed as the % radioactivity found in the pellet:

$$\% \text{uptake} = \frac{\text{cpm (pellet)}}{\text{cpm (pellet)} + \text{cpm (supernatant)}}$$

Table S4: Percentage of internalized ^{67}Ga complexes in *E. coli* K-12 upon incubation in iron sufficient bacterial culture (n=3).

Incubation Time (h)	^{67}Ga -DFO (%)	^{67}Ga -LDFC (%)	^{67}Ga -D1 (%)	^{67}Ga -D2 (%)	^{67}Ga -D3 (%)	^{67}Ga -citrate (%)
0.16	3.8±0.7	3.6±0.9	10.9±6.6	5.6 ±2.4	6.4 ±1.4	3.6 ±1.8
0.33	3.2±0.6	10.0±2.8	6.7 ± 4.9	15.7 ±10.2	24.6 ±8.2	5.0 ±2.4
0.5	4.5±1.2	6.7±2.8	16.6±2.1	16.2 ±5.9	26.5 ±5.1	6.5 ±1.6
1	4.2±1.1	7.5±2.1	15.1±2.8	10.7 ±4.5	5.5 ±1.9	6.1
2	3.3±1.0	7.1±2.8	10.4±6.6	10.3±0.8	9.4±5.6	4.6 ±0.5

Table S5: Percentage of internalized ^{67}Ga complexes in *E. coli* K-12 upon incubation in iron deficient bacterial culture (n=3).

Incubation Time (h)	^{67}Ga -DFO (%)	^{67}Ga -LDFC (%)	^{67}Ga -D1 (%)	^{67}Ga -D2 (%)	^{67}Ga -D3 (%)	^{67}Ga -citrate (%)
0.16	4.2±0.8	21.7±4.2	5.9±1.2	16.8±1.4	18.6±7.4	3.7±0.9
0.33	12±0.8	23.9±4.6	23.4±5.1	14.5±0.7	16.5±0.6	6.9±1.6
0.5	4.9±0.2	13.7±2.1	30.0±8.4	15.3±1.3	22.3±13.5	6.1±1.7
1	5.6±1.5	15.1±3.2	36.6±13.6	15.9±1.3	15.0±8.6	4.9±0.2
2	4.2±1.2	40.9±2.5	13.2±4.1	14.5±5.2	15.3±3.9	6.4±2.1

3.5 Challenge Uptake of ^{67}Ga Labeled Ciprofloxacin-Conjugate (D2) by *E. coli* K-12:

Table S6: Percentage of internalized ^{67}Ga -D2 complex when challenged with 100x Fe-LDFC in *E. coli* K-12 upon incubation in iron deficient bacterial culture.

Incubation Time (h)	^{67}Ga -D2 (%)	^{67}Ga -D2 100x Fe-LDFC (%)	^{67}Ga - citrate (%)
0.16	16.8±1.4	11.4±4.3	3.7±0.9
0.33	14.5±0.7	11.7±3.0	6.9±1.6
0.5	15.3±1.3	10.9±2.9	6.1±1.7
1	15.9±1.3	6.7±1.0	4.9±0.2
2	14.5±5.2	4.5±0.6	6.4±2.1

4. Antibacterial Potency Assays (MIC)

Minimum inhibitory concentrations (MICs) were determined using the broth microdilution method according to the Clinical and Laboratory Standards Institute (CLSI) guidelines.³ All liquids and media were sterilized by autoclaving (220 °C, 1 h) before use. All aqueous solutions and media were prepared using deionized water. Mueller-Hinton broth (MHB) commonly used for antibiotic testing was purchased from Fisher Scientific and used for all MIC assays. MHB is a non-selective and non-differential media which makes it suitable for testing different bacterial strains. It also allows for better diffusion of antibiotics and contains starch that help absorb the toxins produced by bacteria which could interfere with the antibiotics. Mueller-Hinton II broth (cation adjusted) was prepared by adding sterile aqueous solution of 0.41 mL of 1 M Ca²⁺ and 0.15 mL of 1 M Mg²⁺ to 250 mL of MHB. Iron-deficient (-Fe) MHII broth was prepared by adding 4.06 mL of a 1 mg/mL sterile aq. solution of 2,2'-bipyridine to 250 mL of MHII broth.

Sample preparation

Stock solutions of the testing compounds were prepared in sterilized deionized water. Concentrations of Fe-DFO (ϵ : 2450 M⁻¹cm⁻¹)¹ and Fe-LDFC (ϵ : 2400 M⁻¹cm⁻¹)² were analyzed using UV-Vis spectrophotometry. **D1** and **D2** were also analyzed using UV-Vis spectrophotometry and ciprofloxacin-based ϵ : 15304 M⁻¹cm⁻¹ was used for calculating the stock concentrations. Concentrations of Ga-DFO, Ga-LDFC, Fe-**D1**, Ga-**D1**, Fe-**D2**, Ga-**D2** and Fe-**D3** were analyzed using an ICP-OES. A 10-point standard with respect to gallium and iron was used and lines of best fit were found with R² of 0.999. Sample concentration was determined based on this calibration curve.

4.1 MIC Assays Results with *E. coli*

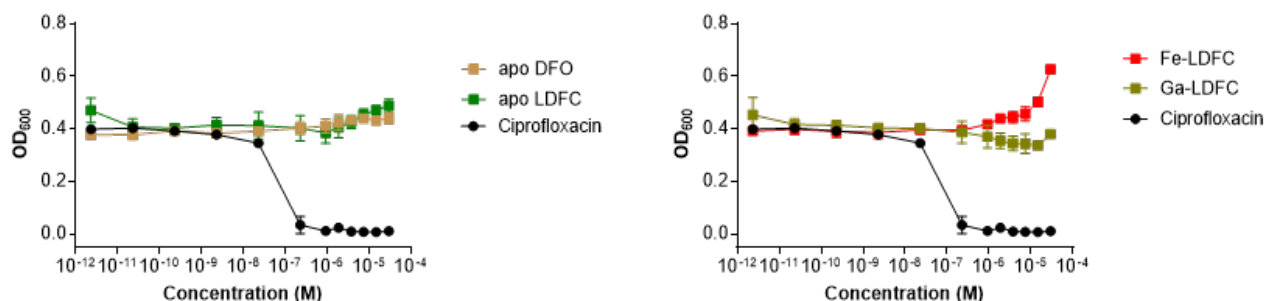


Figure S24: MIC assay of (left) apo DFO, apo LDFC and (right) Fe-LDFC and Ga-LDFC in *E. coli* K12 (n=3). Apo DFO, apo LDFC and Ga-LDFC do not show antibacterial potency against *E. coli* K12, whereas Fe-LDFC acts as growth promoter at concentrations above 10⁻⁵ M.

4.2 Challenge MIC Assays

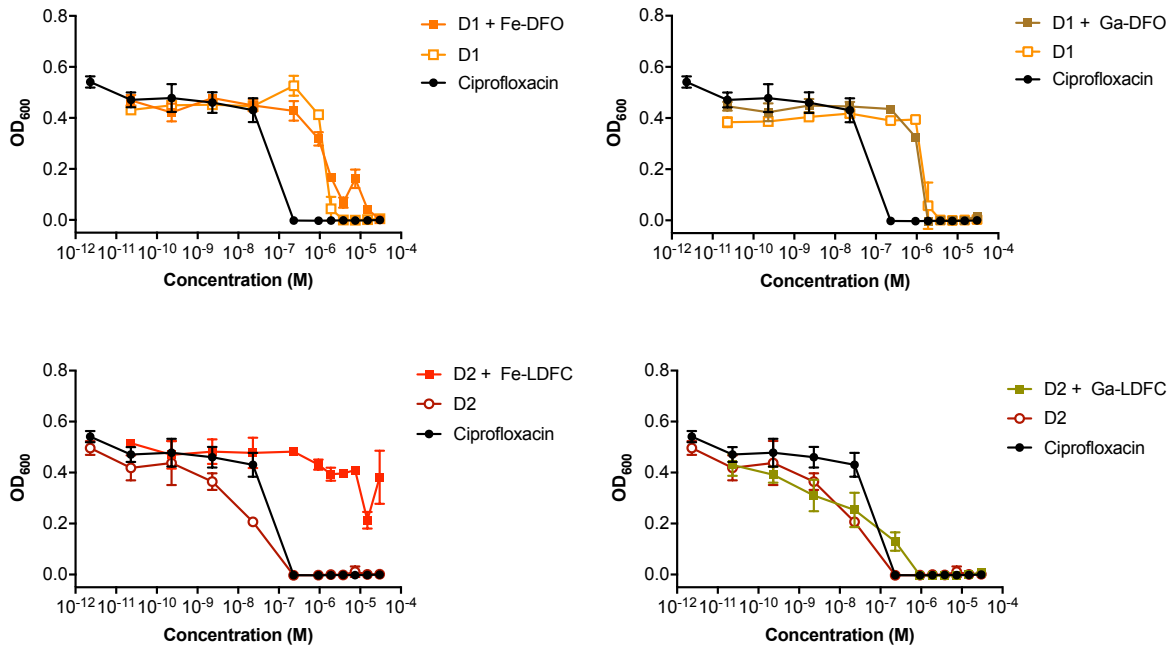


Figure S25: MIC challenge assays of **D1** (top) and **D2** (bottom) in *E. coli* K12 in presence of 100x excess Fe or Ga siderophore (n=3). The Fe-LDFC complex blocks the growth-inhibitory activity of **D2** efficiently, indicating that **D2** is dependent on active transport to the cytoplasm. The same behavior is not observed for **D1**. Ga-complexes do not attenuate the growth inhibitory action of the conjugates as expected, indicating that siderophore-mediated active transport persists.

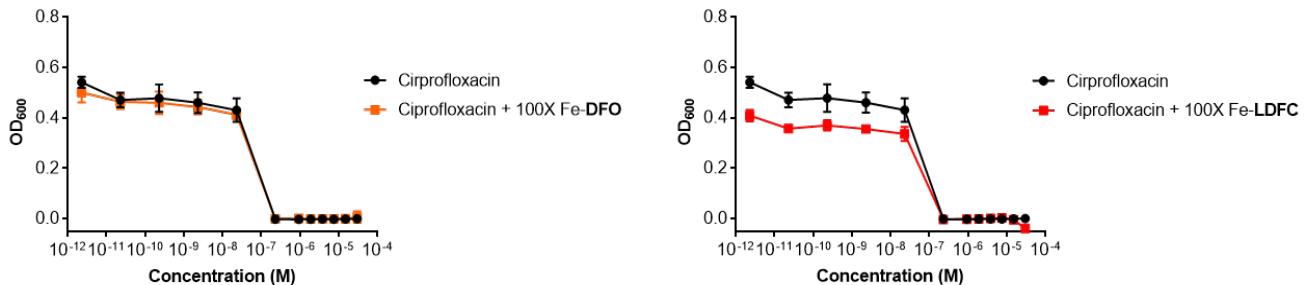


Figure S26: MIC challenge assay of ciprofloxacin in *E. coli* K12 in presence of 100x excess Fe-DFO (**left**) and Fe-LDFC (**right**). The Fe complexes of both DFO and LDFC do not block the growth-inhibitory activity of ciprofloxacin, indicating independent uptake pathway for Fe-siderophores and ciprofloxacin to the cytoplasm. All experiments were carried out in triplicate (n=3).

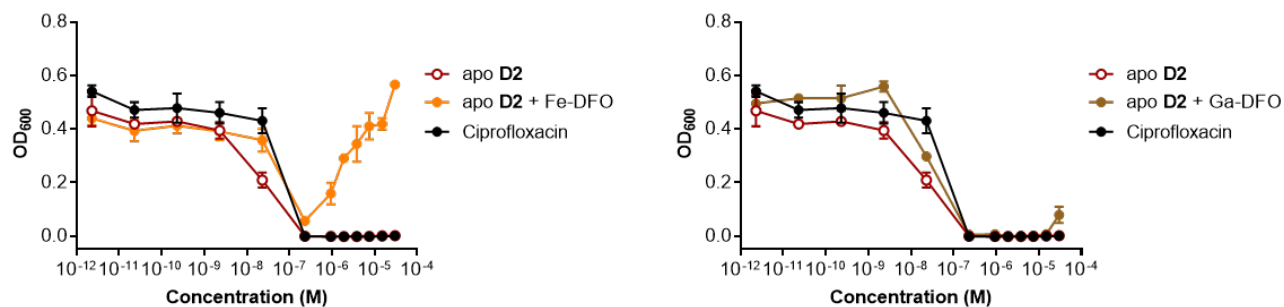


Figure S27: Challenge MIC assay of **D2** in *E. coli* K12 in presence of 100x Fe-DFO (**left**) and 100x Ga-DFO (**right**). 100x Ga-DFO does not block the growth-inhibitory activity of **D2** indicating independent uptake pathway for apo **D2** and Ga-DFO. 100x Fe-DFO does not block the growth-inhibitory activity of **D2** indicating independent uptake pathway at lower concentrations. However, Fe-DFO complex act as growth promoter at concentrations above 10^{-7} M. All experiments were carried out in triplicate (n=3).

4.3 MIC Assay Results with *E. coli* AN193

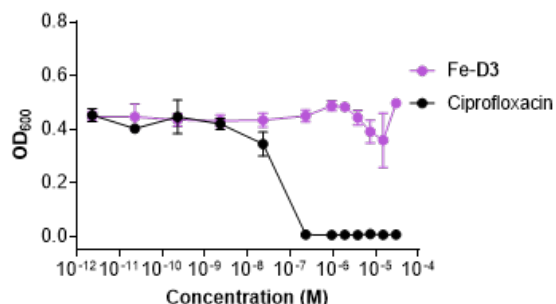


Figure S28: MIC assay of Fe-**D3** in *E. coli* AN193 showing complete attenuation of the growth inhibitory activity of Fe-**D3**.

4.4 MIC Assay Results with *P. aeruginosa* (PA01)

Overnight culture of PA01 was prepared by incubating single colonies of PA01 in 5 mL of iron deficient MHB II (cation adjusted) at 37°C on an incubator shaker for 18 h. Subsequently, the overnight culture was inoculated (1:100) into 10 mL of fresh media and incubated at 37°C until an OD₆₀₀ ~ 0.6 was reached. The culture was further diluted to an OD₆₀₀ of 0.001 for MIC testing. 10 µL solution of testing compound (0.3 mM) was added to the first well of the 96-well plate and serial dilutions were made down each row of the plate. 40 µL of growth media and 50 µL of diluted bacterial inoculum was also added to each well, resulting in a total volume of 100 µL and a concentration gradient of 0.3 x 10⁻⁴ M – 1.56 x 10⁻¹² M. The plates were incubated at 37°C for 18 h. Bacterial growth was determined by measuring the OD₆₀₀ using a plate reader. All experiments were carried out in triplicates.

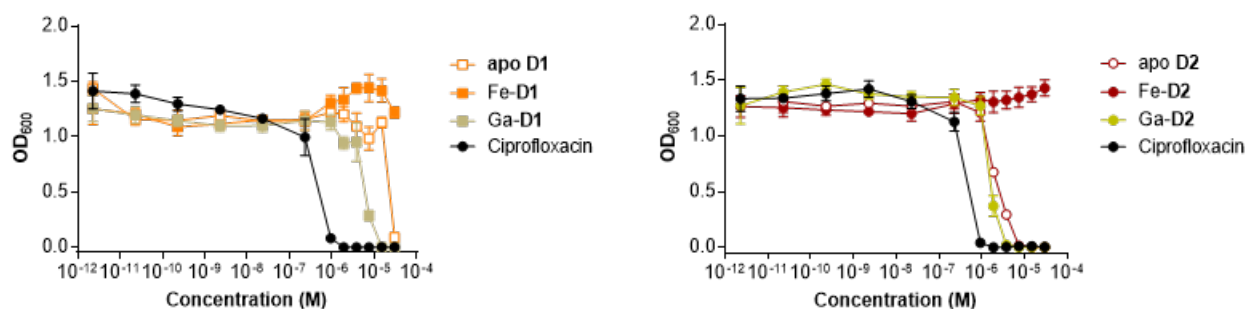


Figure S29: MIC assay of **D1 (left)** and **D2 (right)** in *P. aeruginosa* PA01 show that the Ga-D1/D2 complex exhibits enhanced potency when compared to apo D1/D2, while Fe-D1/D2 complex show no growth inhibition (n=3).

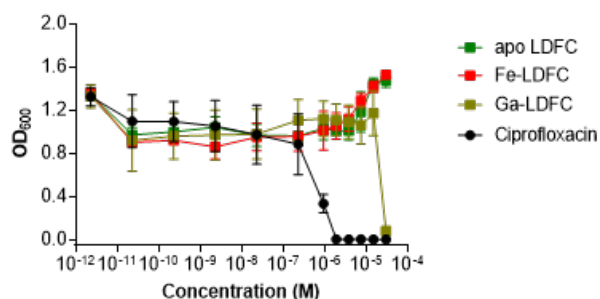


Figure S30: MIC assay of apo LDFC, Fe-LDFC and Ga-LDFC in *P. aeruginosa* PA01. Ga-LDFC is active at highest concentration tested, whereas apo LDFC and Fe-LDFC act as growth promoter at concentrations above 10⁻⁵ M (n=3).

4.5 MIC Assay with *S. aureus* newman (RN4220)

Overnight culture of *S. aureus* newman was prepared by incubating single colonies in 5 mL of iron deficient MHB II (cation adjusted) at 37°C on an incubator shaker for 18 h. Subsequently, the overnight culture was inoculated (1:100) into 10 mL of fresh media and incubated at 37°C until an OD₆₀₀ ~ 0.6 was reached. The culture was further diluted to an OD₆₀₀ of 0.001 for MIC testing. 10 µL solution of testing compound (0.3 mM) was added to the first well of the 96-well plate and serial dilutions were made down each row of the plate. 40 µL of growth media and 50 µL of diluted bacterial inoculum was also added to each well resulting in a total volume of 100 µL and a concentration gradient of 0.3 x 10⁻⁴ M – 1.56 x 10⁻¹² M. The plates were incubated at 37°C for 15 h. Bacterial growth was determined by measuring the OD₆₀₀ using a plate reader. All experiments were carried out in triplicates.

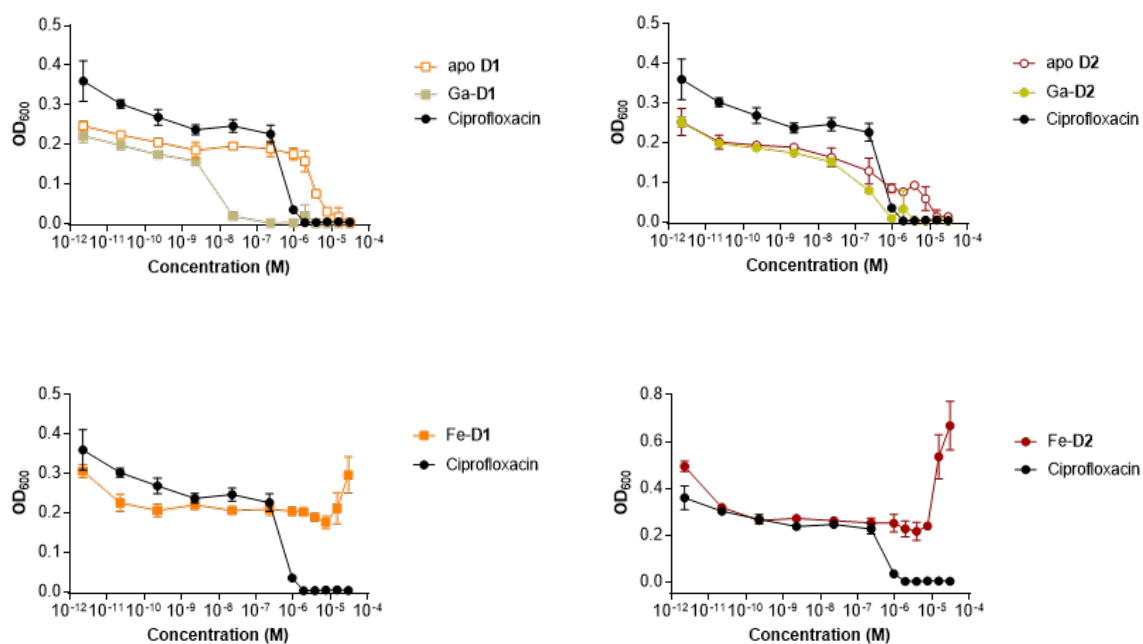


Figure S31: MIC assay of D1 (top left) and D2 (top right) in *S. aureus* RN4220 show that the Ga-D1/D2 complex exhibits enhanced potency when compared to apo D1/D2, while Fe-D1 (bottom left) and Fe-D2 (bottom right) complex act as growth promoter at concentrations above 10⁻⁵ M (n=3).

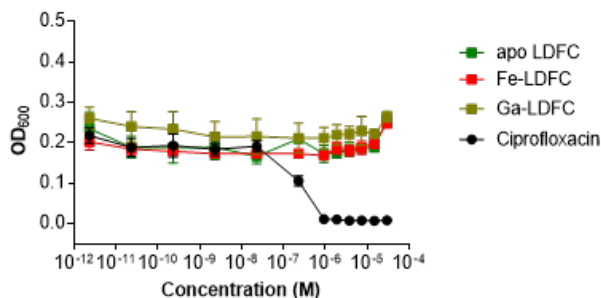


Figure S32: MIC assay of apo LDFC, Fe-LDFC and Ga-LDFC in *S. aureus* RN4220. Apo LDFC and its Fe and Ga complex show no activity and acts as growth promoter at concentrations above 10^{-5} M (n=3).

4.6 MIC Assay Results with *K. pneumoniae* CRE-11

Overnight culture of *K. pneumoniae* was prepared by incubating single colonies in 5 mL of iron deficient MHB II (cation adjusted) at 37°C on an incubator shaker for 18 h. Subsequently, the overnight culture was inoculated (1:100) into 5 mL of fresh media and incubated at 37°C until an $OD_{600} \sim 0.6$ was reached. The culture was further diluted to an OD_{600} of 0.001 for MIC testing. 10 μ L solution of testing compound (0.3 mM) was added to the first well of the 96-well plate and serial dilutions were made down each row of the plate. 40 μ L of growth media and 50 μ L of diluted bacterial inoculum was also added to each well resulting in a total volume of 100 μ L and a concentration gradient of 10^{-4} M – 1.04×10^{-12} M. The plates were incubated at 37°C for 13 h. Bacterial growth was determined by measuring the OD_{600} using a plate reader. All experiments were carried out in triplicates.

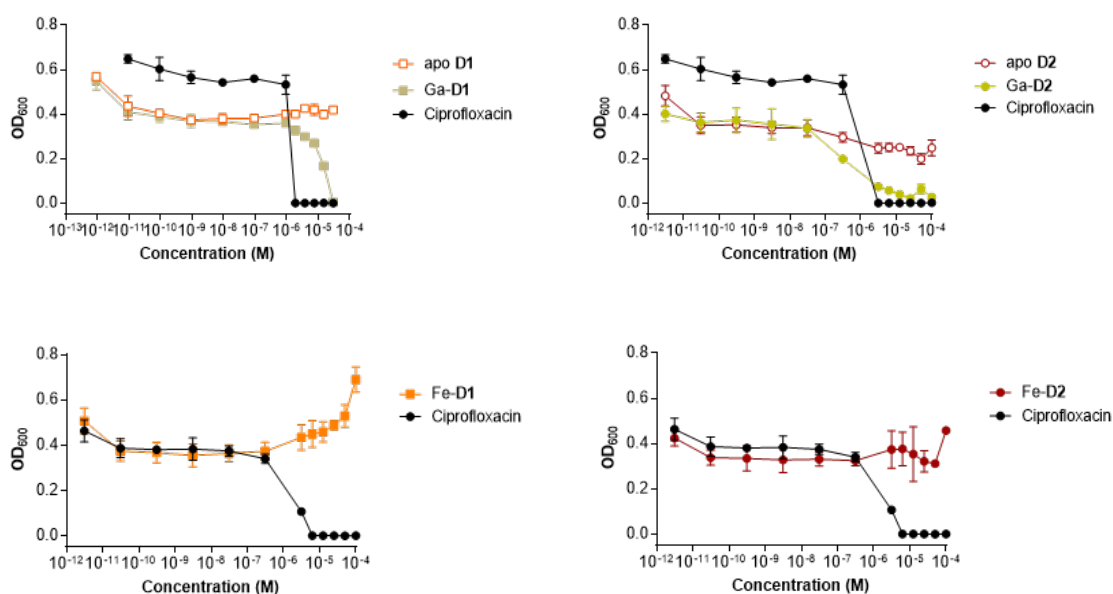


Figure S33: MIC assay of D1 (top left) and D2 (top right) in *K. pneumoniae* CRE-11 show that the Ga-D1/D2 complex exhibits enhanced potency when compared to apo-D1/D2, while Fe-D1 (bottom left) and Fe-D2 (bottom right) complex act as growth promoter at concentrations above 10^{-6} M (n=3).

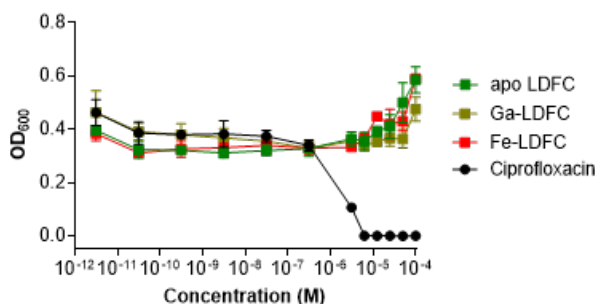


Figure S34: MIC assay of apo LDFC, Fe-LDFC and Ga-LDFC in *K. pneumoniae* CRE-11. Apo LDFC and its Fe and Ga complex show no activity and acts as growth promoter at concentrations above 10^{-6} M (n=3).

4.6 MIC Assay Results with Fe-D3 (albomycin) in Different Bacterial S trains

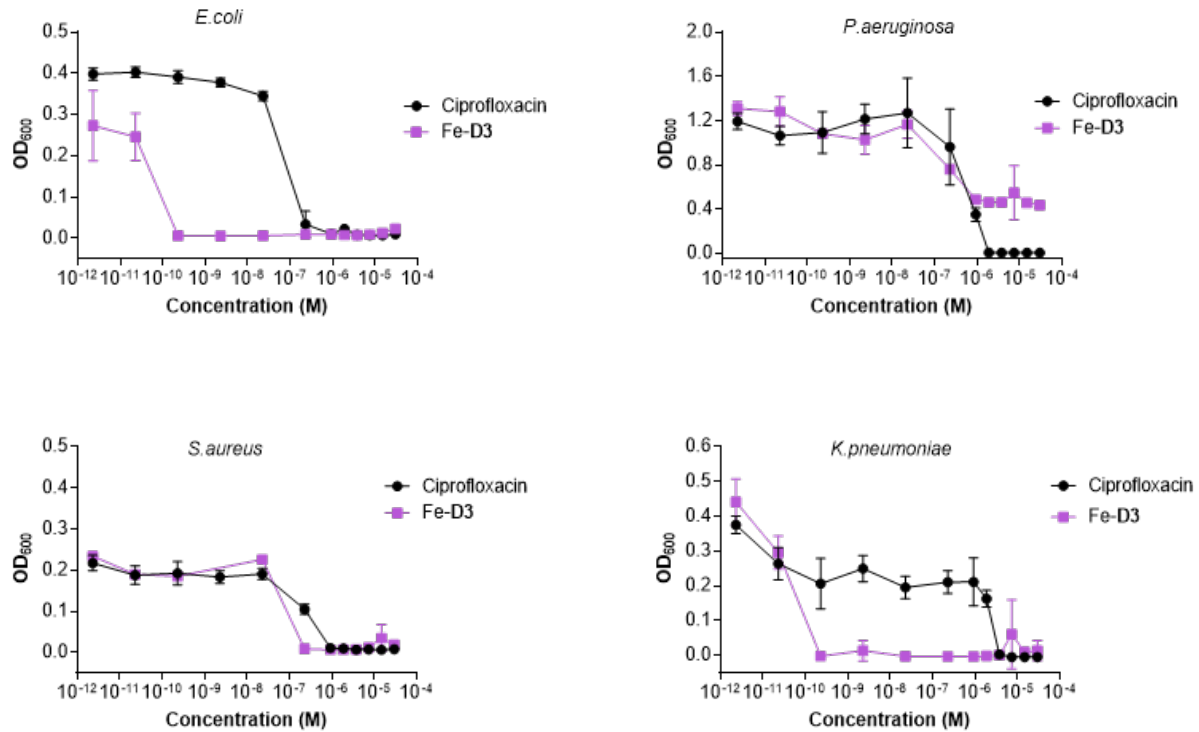


Figure S35: MIC assay of Fe-D3 in *E. coli* K-12, *P. aeruginosa* PA01, *S. aureus* RN4220 and *K. pneumoniae* CRE-11 (n=3).

Table S7: MIC₉₀ values of literature ciprofloxacin-siderophore drug conjugates and novel **D1** and **D2** conjugates reported.

Compound	MIC₉₀ (μM) <i>E.coli</i> (K-12, assay conditions)	Maximum potency MIC₉₀ in μM (strain)	Ref.
Ciprofloxacin	0.23 (MHII – Fe, 2% DMSO, 18h, 37 °C)	0.015 (<i>E. coli</i> ATCC 25922)	4
Ent-cipro	> 128 (M9 media, 1% DMSO, 30°C, 20h)	0.1 (<i>E.coli</i> UTI89)	5
Ent-PEG ₃ -cipro	>10 (M9 media, 1% DMSO, 30°C, 20h)	10 (<i>E.coli</i> UTI89)	5
Ent-ss-cipro	> 10 (M9 media, 1% DMSO, 30°C, 20h)	0.1 (<i>E.coli</i> B)	6
DFO-trimethyl lock-Cipro	n.a.	1 (<i>E. aerogenes</i> ATCC 35029) 1 (<i>E. coli</i> ATCC 25922)	7
Danoxamine (n=1) conjugate (1c)	n.a	2 (<i>E. coli</i> ATCC 25922)	8
Danoxamine (n=2) conjugate (2c)	n.a.	2 (<i>E. coli</i> ATCC 25922)	8
Danoxamine (n=3) conjugate(3c)	>128 (MHII – Fe, 2% DMSO, 18h, 37 °C)	1 (<i>S. aureus</i> SG 511)	8
Biscatecholate mixed ligand siderophore	> 128 (MHII – Fe, 2% DMSO, 18h, 37 °C)		4
121,3-c- ciprofloxacin	n.a.	490 (<i>E. coli</i> NCTC 10418)	9
1,3-c-Gly ciprofloxacin	n.a.	220 (<i>E. coli</i> NCTC 10418)	9
1,3-c-Ava- ciprofloxacin	n.a.	>1000 (<i>E. coli</i> NCTC 10418)	9
<i>apo-D2</i>	0.23 ((MHII – Fe, 18h, 37 °C)		<i>This work</i>
<i>Fe-D2</i>	0.94 (MHII – Fe, 18h, 37 °C)		<i>This work</i>
<i>Ga-D2</i>	0.23 (MHII – Fe, 18h, 37 °C)		<i>This work</i>
<i>apo-D1</i>	3.8 (MHII – Fe, < 1% DMSO, 18h, 37 °C)		<i>This work</i>
<i>Fe-D1</i>	10 (MHII – Fe, 18h, 37 °C)		<i>This work</i>
<i>Ga-D1</i>	3.8 (MHII – Fe, 18h, 37 °C)		<i>This work</i>

5. Animal Studies

5.1 Biodistribution

Table S8: Biodistribution of ^{67}Ga conjugates at 1 h p.i. (n=3).

Organ	$^{67}\text{Ga-D1}$ (%ID/g)	$^{67}\text{Ga-D2}$ (%ID/g)	$^{67}\text{Ga-D3}$ (%ID/g)	$^{67}\text{Ga-citrate}$ (%ID/g)
Blood	12.9±6.5	9.3±0.7	5.7±0.5	16.6±13.0
Heart	2.9±0.2	3.1±0.1	2.1±0.1	6.0±4.0
Lung	7.2±3.5	6.2±0.3	16.9±5.7	10.9±8.2
Liver	12.3±2.2	3.0±0.4	7.4±0.6	3.8±1.8
Spleen	7.5±0.3	3.2±0.1	2.6±1.1	3.7±2.6
Kidney	4.3±0.09	10.1±1.3	3.1±0.7	8.0±4.9
Small intestine	3.1±0.5	3.1±0.1	1.2±0.6	4.1±2.8
Muscle	1.1±0.03	1.4±0.05	0.5±0.06	1.7±0.9
Bone	4.5±0.5	6.1±0.8	1.5±1.06	3.4±2.4
Urine	40.2±26.9	54.0±21.4	12.3±5.2	26.7±21.7

5.2 Metabolite Analysis

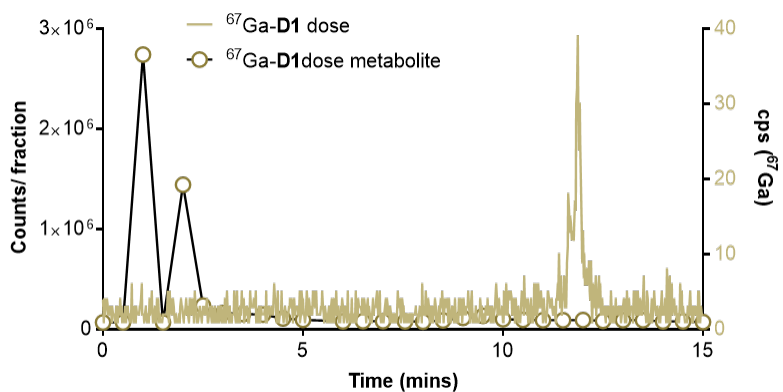


Figure S36: Metabolite analysis of $^{67}\text{Ga-D1}$ complex in the urine 1 hour post injection.

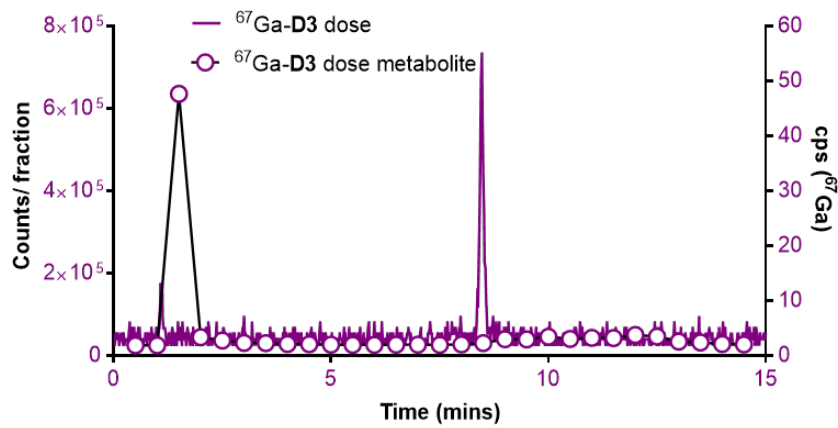


Figure S37: Metabolite analysis of $^{67}\text{Ga-D3}$ complex in the urine 1 hour post injection.

6. References

1. Monzyk, B., & Crumbliss, A. L. (1982). Kinetics and mechanism of the stepwise dissociation of iron (III) from ferrioxamine B in aqueous acid. *J. Am. Chem. Soc.*, *104*(18), 4921-4929.
2. Emery, T., & Hoffer, P. B. (1980). Siderophore-mediated mechanism of gallium uptake demonstrated in the microorganism *Ustilago sphaerogena*. *J. Nucl. Med.*, *21*(10), 935-939.
3. CLSI. Methods for dilution antimicrobial susceptibility tests for bacteria that grow aerobically. 8th ed. Villanova, PA: 2009.
4. Wencewicz, T. A., & Miller, M. J. (2013). Biscatecholate–monohydroxamate mixed ligand siderophore–carbacephalosporin conjugates are selective sideromycin antibiotics that target *Acinetobacter baumannii*. *J. Med. Chem.*, *56*(10), 4044-4052.
5. Neumann, W., Sassone-Corsi, M., Raffatellu, M., & Nolan, E. M. (2018). Esterase-catalyzed siderophore hydrolysis activates an enterobactin–ciprofloxacin conjugate and confers targeted antibacterial activity. *J. Am. Chem. Soc.*, *140*(15), 5193-5201.
6. Neumann, W., & Nolan, E. M. (2018). Evaluation of a reducible disulfide linker for siderophore-mediated delivery of antibiotics. *J. Biol. Inorg. Chem.* *23*(7), 1025-1036.
7. Ji, C., & Miller, M. J. (2012). Chemical syntheses and in vitro antibacterial activity of two desferrioxamine B-ciprofloxacin conjugates with potential esterase and phosphatase triggered drug release linkers. *Bioorg. Med. Chem.*, *20*(12), 3828-3836.
8. Wencewicz, T. A., Long, T. E., Möllmann, U., & Miller, M. J. (2013). Trihydroxamate siderophore–fluoroquinolone conjugates are selective sideromycin antibiotics that target *Staphylococcus aureus*. *Bioconjugate Chem.*, *24*(3), 473-486.
9. Milner, S. J., Snelling, A. M., Kerr, K. G., Abd-El-Aziz, A., Thomas, G. H., Hubbard, R. E., ... & Duhme-Klair, A. K. (2014). Probing linker design in citric acid–ciprofloxacin conjugates. *Bioorg. Med. Chem.*, *22*(16), 4499-4505
10. Lin, Z, Xu, X. Zhao S., Yang X., Guo J., Zhang, Q, Jing C., Chen, S. He, Y. (2018) Total Synthesis and antimicrobial evaluation of natural albomycins against clinical pathogens. *Nature Comm.*, *9*, 3445.